Photopolymerization of Thin Polycrystalline Diacetylene Films and Quenching of the Precursor Excited State

Sylvie Spagnoli, Jean-Louis Fave, Michel Schott

Photopolymerization of Thin Polycrystalline Diacetylene Films and Quenching of the Precursor Excited State

Sylvie Spagnoli,*,† Jean-Louis Fave,‡ and Michel Schott*,‡

†Laboratoire Interdisciplinaire de Physique (LIPhy), UMR 5588, Université Grenoble1/CNRS, BP87 38402 Saint Martin d'Hères, France

‡Institut des Nanosciences de Paris, UMR 7588-CNRS, UPMC (Université Pierre et Marie Curie), case 840, 4 Place Jussieu, 75252 Paris, Cedex 05, France

ABSTRACT: Microcrystalline films of the diacetylenes 4BCMU and 3BCMU were prepared by vacuum evaporation and polymerized by UV irradiation. A method for determining the absolute polymer content X in films has been developed. In 4BCMU the reaction rate is strongly decreased beyond $X \sim 0.3$. Existing models fail to fit the kinetics. A numerical model based on quenching of the monomer excited state, the initiation precursor, by energy transfer to a nearby existing chain is developed and quantitatively fits the kinetics. Such quenching may occur in any diacetylene solid, so that one should not assume that an apparent saturation of the absorbance of a film corresponds to complete polymerization. 3BCMU is less reactive and briefly compared to 4BCMU.

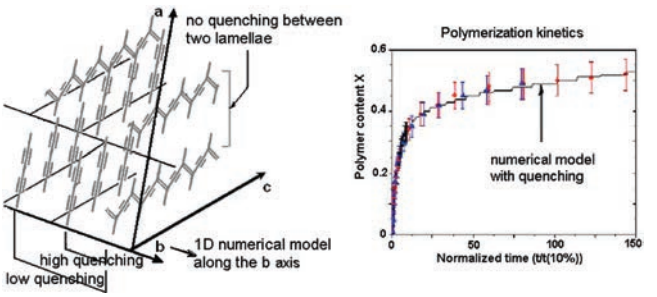

INTRODUCTION

Polydiacetylenes (PDA) are a class of conjugated polymers of special interest since they are formed in the solid crystalline state of their parent monomer diacetylene (DA) by a topochemical reaction,[1−3] so that several of them can be obtained as good quality polymer single crystals of macroscopic size,[4] and serve as model systems for the electronic properties of conjugated polymers.[5] The spectroscopy of isolated chains of these PDA in their single crystal monomer matrix has been studied, and it has been showed that they behave as perfect quasi-1D systems[6] on which the exciton is spatially coherent over the whole chain length at low temperature (micrometers), being an electronic state of the whole chain.[7,8]

Another property of interest of some PDA is that several electronic structures exist for these conjugated polymer chains, evidenced by different colors of the solid polymer, the most frequent being "blue " and " red ", the latter but not the former being luminescent, with high quantum yields at low temperature.[9−11] The origin of these differences, and the corresponding structural differences which must exist, are still a matter of debate,[12] and one of us has recently provided computational evidence for a model where blue chains are planar and red ones are twisted (nonplanar).[13] A PDA can make transitions between colors, either reversible or irreversible; poly-4B for instance shows such an irreversible blue to red transition. This property is currently put to use to develop biological or chemical sensors, mostly using LB films, membranes, or vesicles.[14,15] PDA LB films are almost always prepared by UV polymerization, which is much easier to implement than γ-irradiation.

In UV-photopolymerization of DA into PDA, chain initiation and propagation steps at low temperature and small polymer content have been studied in details using single crystals (see, for instance, refs 16 and 17), but the overall reaction up to completion is much less well understood. This is, at least in part, due to the fact that polymer chains themselves absorb at wavelengths used for photoinitiation, so that distribution of initiation events within the volume of a crystal becomes quickly very inhomogeneous, strongly distorting the kinetics.[18,19] This problem is absent in thermal or γ-ray-induced polymerizations where excitation is a bulk process. There are few kinetic studies of photoolymerization of LB multilayers[20,21] and Langmuir monolayers.[22] However, the absolute polymer contents X are almost never determined. Incomplete polymerization is sometimes mentioned[23,24] but is considered to be of structural origin, related either to a phase change[24] or to the existence of two types of monomers that cannot both be in a topochemically favorable geometry at the same time.[23] Apparently, it was generally assumed that the quasi-stationary value reached at long times is $X = 1$. A blue to red transition often occurs during polymerization which complicates further the kinetic scheme.

In this paper we wish to address some open questions relative to DA photopolymerization, considering the (most frequent) case of homogeneous reaction where the reacting solid remains a mixed DA−PDA crystal throughout. As reaction proceeds, several phenomena may conceivably modify the reactivity, beyond the

obvious effect of a decreasing amount of unreacted monomer available for the reaction:

(a) Existing chains can block propagation of new chains, hence a shortening of average chain length.

(b) If the distance in the crystal between two monomers forming the reaction center is not equal to the equilibrium repeat distance of the polymer chains, existing chains will generate an internal stress in the mixed crystal and so will progressively force the distance between reacting monomers to become close or equal to the repeat unit polymer length. This would in principle increase reactivity.

(c) Side groups packing may change and become more or less favorable, even finally blocking the reaction.

(d) Photopolymerization initiation comes from an electronically excited state of the monomer. A neighboring chain may quench this state leading to decreased reactivity.

(e) As already mentioned, the polymer formed in early stages of the reaction will act in thick enough samples as an internal filter and block penetration of UV light in depth, resulting in very inhomogeneous polymer content. A striking example is the DA pTS where thermal and γ-polymerization kinetics show an induction period (see, for example, ref 19) while UV reaction apparently does not.[18] This may be qualitatively explained by an internal filter effect,[19] but clearly the experimental kinetics are hardly tractable.

Issues (a)−(c) were theoretically addressed in very important papers by Baughman.[25,26] This author in fact had in mind the thermal polymerization of bulk pTS and aimed to explain its sigmoïdal kinetics, but he suggested that his theory is also relevant to other situations.

The diacetylenes (DA) chosen for the present work are known as 3BCMU and 4BCMU (abbreviated below 3B and 4B) of side group formula $-(CH_2)_n-OCONH-CH_2-COOC_4H_9$ with $n = 3$ for 3B and $n = 4$ for 4B. They form lamellar crystals,[27−30] so they are crystalline analogues to DA Langmuir−Blodgett films. The corresponding PDA have been much studied, partly because they are among the few soluble PDA.[31]

In their case the longitudinal mismatch between monomer and polymer, so important in pTS, is nearly absent (in 3B) or small (in 4B) so problem (b) will not be important. As we shall see, the choice of studying microcrystalline films also eliminates problems (a) and (e).

On the other hand, several specific problems arise in γ-ray polymerization of 3B and 4B (information on their UV-induced reactivity is limited[32−34]):

(f) 4B is said to γ-polymerize completely[35] with a very high initial reactivity[36] and a rapid slowing down beyond a polymer content $X \sim 0.1$. One then expects one or several of the above processes to be important.

(g) 3B is initially almost as reactive as 4B under γ-irradiation,[36] but its reactivity decreases strongly beyond $X \sim 0.5$:[35] no bulk poly-3B has ever been prepared. Moreover, 3B reactivity to UV is much smaller than its γ-reactivity, even at very small polymer content. And this is so although the reactive center geometry is apparently optimal.[29]

3B and 4B are not thermally reactive, and the polymers have to be prepared by irradiation, using UV photons or γ-rays. While their overall γ-ray polymerization kinetics has been studied,[19,35] this has been done for UV photons only for 4B and only in part.[32] The UV study is difficult to perform with bulk monomer crystals due to the internal filter effect. We recently studied the early stages of the UV polymerization, up to a few % polymer, where this difficulty is negligible.[34] To circumvent the difficulty of absorption by polymer chains, we have prepared and studied in the present work well-characterized microcrystalline films of both materials, thin enough for their optical density in the UV to be less than 0.2 at all polymer contents. In both materials, chains remain at all X in the "blue" PDA phase (see, for instance, ref 5). Conditions for achieving the blue to red color transition in these films will be discussed in a further paper.

Since 3B and 4B behave very differently in photopolymerization, they will be discussed separately, after presentation of the experimental methods. It will be shown that for the photopolymerization kinetics of 4B the quenching of the initiation reaction by existing chains is a limiting process.

EXPERIMENTAL METHODS

Substrate Preparation. Films were deposited by vacuum evaporation onto glass, with an average roughness (measured by AFM) smaller than 1 nm. Substrates were cleaned ultrasonically at room temperature just before use, in four steps: 15 min in a 1% detergent solution in deionized water, 5 min rinsing in water, 15 min in acetone, 5 min rinsing in water, and finally dried at 60 °C in air. This procedure ensures reproducible substrate surface condition but is not claimed to produce a perfectly clean surface.

Monomer Film Deposition. 3B and 4B were synthetized in the laboratory by the usual reaction of the corresponding diynediol with butyl isocyanatoacetate.[31] Evaporations were performed at a base pressure of $(2-3) \times 10^{-7}$ Torr on substrates at room temperature, with deposition rates 0.1−0.5 Å/s so the time for depositing a monolayer (a single lamella) was usually of the order of minutes. Up to 16 films could be prepared simultaneously, making possible comparison of kinetics in different conditions. The substrate holder was rotated around a vertical axis during deposition in order to have as equal as possible thicknesses on all substrates; this was experimentally verified (see below). 30−90 mg of monomer powder was placed in a cylindrical quartz crucible tightly inserted in a cylindrical temperature controlled oven and heated to about 110 °C. The temperature was regulated using a thermocouple pressed against the crucible bottom. Rates and thicknesses were measured using a vibrating quartz balance.

Characterization. To deduce a polymer content from an optical density, the film thickness and the polymer absorption coefficient in the films α_{fp} (which may differ from that in single polymer crystals α_p) have to be known. Determinations of α_{fp} will be presented separately for 4B and 3B.

Determination of Film Thickness. During evaporation, the average thickness measured by the vibrating quartz differs from the true sample thickness since substrate and quartz are not at the same position, so a geometrical correction has to be applied. This correction is not negligible since in our setup it amounts to ∼20%. This factor was calculated but may vary slightly, so actual sample thicknesses were directly measured for each deposition run. Two methods were considered. The number densities N_C of C atoms per unit surface were measured by Nuclear Reaction Analysis (NRA) using the nuclear reaction $^{12}C(d,p)^{13}C$ at 975 keV on the van de Graaff accelerator at the SAFIR facility at INSP, and the depth of trenches cut through the films was measured by profilometry.

1. In NRA a deuton dose of 0.5 μC was enough to yield N_C values averaged over the 5 mm^2 irradiated surface with a statistical uncertainty of ∼1%, except for the thinnest sample (50 nm) and without any measurable loss of C atoms due to radiation damage. The absence of C loss was verified by applying the deuton dose in steps of 100 nC with beam current of one to few nA, separated by a waiting time to allow the sample to return to room temperature if any heating had occurred; no

variation beyond the purely statistical ones was observed from dose to dose. The true uncertainty on thickness is not statistical but is due to the imperfect knowledge of the nuclear reaction cross sections. Since no stable C standard exists, an O standard is used and the ratio 5.56 of its cross section to that of the C reaction is known to ±5% only[37] so relative thicknesses are more accurately known than absolute ones. The thickness is then calculated using the known monomer crystal densities $\rho = 1.14\ g/cm^3$ for 4B and $\rho = 1.21\ g/cm^3$ for 3B.[29] During polymerization it varies by 1.6% only in 4B.[30] The corresponding value for 3B is not known. Several areas on the same film and several sets of two films from the same batch were measured to check that they indeed have the same uniform thickness.

2. Profilometry is in principle a direct and local determination. However, it was found that reliable measurements could only be obtained by using a broad tip (a diamond sphere of diameter 12.5 μm) and under light weight ($\leq$1 mg) (Veeco Dektak150). Thicknesses so obtained are equal to or slightly smaller than the NRA values on the same film. With sharper tips smaller thicknesses were always measured however without any observable permanent damage of the film. We conjecture that this apparent variation with contact size is due to elastic deformation of the material: both 3B and 4B are lamellar crystals and are easily deformed in the direction perpendicular to the lamellae. Observations of similar deformations have been made in STM experiments on graphite (see among many other works ref 38). With higher weights wear and/or plastic deformation occurred, and repeated measurements at the same position yielded constantly decreasing thicknesses.

Profilometry was therefore considered less reliable, and NRA determined thicknesses were used. The thicknesses of the studied films were in the range 50−250 nm.

Film roughness was measured by AFM (Nanoscope III). They are always about 10% of the total film thickness. This suggests that films grow three-dimensionally and not layer by layer.

Crystallinity and Morphology of the Films. The mere fact that they polymerize and have the same spectroscopic properties as bulk polymer crystals is a proof that these films are crystalline and a strong indication that their crystal structure is the same as the bulk polymer. AFM images of the film surfaces show flat and more or less rectangular terraces of submicrometer size with step heights of 2.7 nm (respectively 3 nm) or small multiples of that; this is the thickness of a single lamella in bulk 4B (respectively 3B) monomers[29] and poly-4B crystals.[30] Thus, the films seem to be a compact set of crystallites all having their *a*-axis perpendicular to the surface, and the polymer chains randomly oriented within the surface plane (the absorption spectra are unpolarized) for monomers arrangement details (see Scheme1). No epitaxy is expected on the chosen substrates. The analysis of absorption spectra (see below) will show that the crystal quality of monomer microcrystals is similar to that of slowly grown large single crystals. This shows that nucleation is easy. This was not obvious considering that monomers are large, long, and flexible molecules. The fact that each monomer is linked to two others, each by two H bonds, may explain this facile nucleation.

Crystallite Sizes and Polymer Chains Length. The number η_p of monomers included in a chain per absorbed photon can be determined from the kinetics, but the initiation probability η_i cannot, unless an average polymerization index *N* or chain molecular weight *M* is known. In a 4B or 3B single crystal, polymer chains can grow to lengths >10 μm;[7] therefore, in a polycrystalline film with small enough grain size, as here, the chain length is limited by the crystallite size and not by the presence of other chains: this remains so during the whole polymerization. Two methods were then used to obtain information about *N*.

AFM images allow determination of crystallite sizes at the surface, but whether or not they extend throughout the film thickness is not known. Average sizes around 300 nm were consistently observed, but it is difficult to prove that the studied regions were a representative set although they were in principle chosen at random. These sizes are similar to the size of the domains in several studies of PDA LB films.[39,40]

Scheme 1. (left) A 3D View of a Monomer−Polymer Mixed Crystal Showing the Various Quenching Situations Considered. The 1D Numerical Model Corresponds to the Projection of the (b,c) Plane onto the b Axis. (right) Projection of the Structure on the (a,b) Plane, Showing the Packing of the Lamellae and of Molecules within a Lamella[a]

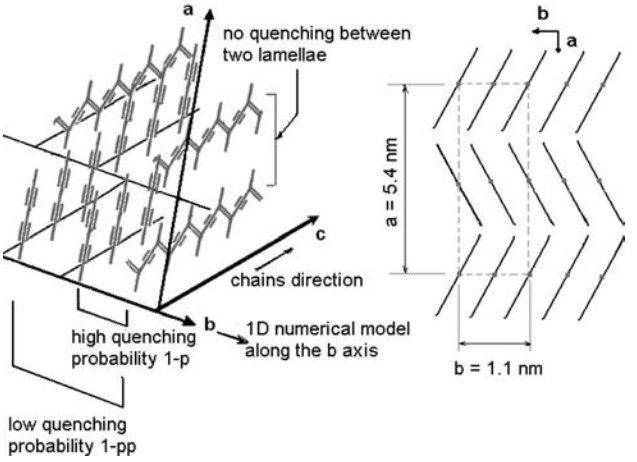

[a] Polymer chains project on the center of the segments representing a molecule.

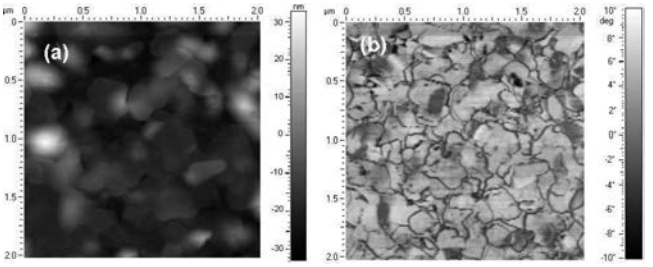

Figure 1. AFM images of two 4B evaporated films: (a) thickness 120 nm photopolymerized film, topographic image; (b) thickness 350 nm, 4B monomer, phase image. The crystallographic direction **a** is perpendicular to this image.

GPC determination of the molecular weight distribution is a direct and accurate method. 20 cm^2 of film with 250 nm thickness was prepared and polymerized in order to obtain enough polymer to prepare solutions of sufficient concentrations. 0.12 mg/mL solutions of poly-4B in THF were studied on multiple detection columns with detectors for refractive index, light scattering, and viscosity, yielding absolute molecular mass values $M_w = 3.02 \times 10^5$, $M_n = 1.91 \times 10^5$, and $M_w/M_n \simeq 1.65$. Hence, a polymerization index $N_w \simeq 630$ using the monomer mass of 508 and an average chain length in the crystallites ≃300 nm, as measured on AFM images (Figure 1): chains always grow to the full size of the crystallite.

It is worth mentioning that poly-4B masses were also computed using the polystyrene calibration. The masses so obtained were larger by a factor 1.7 than the true masses given above. This factor is slightly smaller than the value previously obtained for masses of several millions, 2.15.[41] The difference may be related to the fact that at $M \sim 3 \times 10^5$ a poly-4B chain is still far from the infinite chain limit.[42] Similar observations have been made on other conjugated polymers.[43] Most poly-4B used in the literature were characterized using a polystyrene calibration, so the quoted masses were overestimated by a factor between 1.5 and more than 2 depending on the masses. We do not claim that this factor is valid for all soluble PDA; for instance, the polystyrene calibration has been

found to be approximately correct for poly-TS12.[44] The difference may be related to the possibility or not for the side groups to form H-bonds with each other or with the solvent or the stationary phase. If so, the factor found here is probably at least approximately valid for other polymers of the BCMU family, on which the larger part of the work on soluble PDA has been performed.

Photopolymerization Method. Photopolymerizations were performed at or around room temperature (15−29 °C), either in a Cary 5000 spectrophotometer using 225 nm photons (spectral bandwidth 5 nm) and a flux $\phi = 1.93 \times 10^{11}$ cm^{-2} s^{-1} measured using a calibrated detector (Ophir PD300-UV) or with the polychromatic beam from a 450 W Xe lamp, selecting the wavelength range 230−270 nm by a 45° reflection dielectric mirror for unpolarized light (CVI-Melles Griot mirror KRF-2037−45-UNP), with approximately constant flux over several cm^2, larger than our samples size. The corresponding photon flux was ∼370 times that in the Cary. The chosen wavelengths are similar to those commonly used for LB film polymerization.

A fairly complete kinetics can be obtained with the Xe lamp in less than 3 h of irradiation, but the reaction at initial stages is too fast, so irradiations at lower flux in the Cary were used for studying these early stages.

Polymerization is not affected by the presence of oxygen, as already known for solid-state polymerization of similar compounds.[45] All samples were therefore irradiated in air.

The polymerized area in the Cary had an ovoid shape, surface ∼0.6 cm^2. Polymerization was visually homogeneous throughout that region. Homogeneity was checked by recording absorption spectra through a 0.2 × 2 mm^2 slit at 10 different positions of a film: the recorded optical densities did not vary by more than ±3.5% from point to point. This indicates that both photon flux and film thickness are constant over the whole irradiated surface. The spectra used for kinetic studies in the spectrometer were recorded without moving the sample, throughout the reaction process, using a 1 × 4 mm central region of the polymerized area and a spectral resolution of 1 nm.

Monomer absorbances at 225 nm were calculated using absorption coefficients measured on monomer single crystals at room temperature: $\alpha_m \simeq 800$ cm^{-1} for 4B and $\alpha_m \simeq 1650$ cm^{-1} for 3B.[34] These values are similar to those found for solutions of other DA such as hexadiynediol[46] or other diynes.[47,46] The difference between 3B and 4B is likely due to different angles between the transition dipole and the substrate plane, but this cannot be proved since the atomic positions in the 4B monomer structure are not known.[29]

RESULTS AND DISCUSSION

Photopolymerization of 4BCMU Thin Films. *Absorption Coefficient of the Polymer in the Films.* The actual polymer content can be deduced from the measured optical density of the film once the absorption coefficient α_{fp} of the polymer in the film is known (by this we mean the absorption coefficient that a completely polymerized film would have). So, the light I_{trans} transmitted through a film of thickness d with a polymer content X is $I_{trans} = I_0 \exp(-\alpha_{fp} X d)$. Note that the optical densities OD used below or shown on the figures correspond to $OD = \log(I_0/I_{trans})$.

The measurement is done for a film with a certain polymer content. The so obtained values may or may not be valid for all X, depending on changes of the shape of absorption spectra with X. This will be discussed further below. It will be shown that for 4B corrections are small or negligible.

$\alpha_{fp}^{(0)}$ at the peak near 620 nm (see Figures 2 and 3) and $\alpha_{fp}^{(D)}$ at the vibronic peak near 580 nm were determined using a method that does not require knowledge of the thickness d or polymer

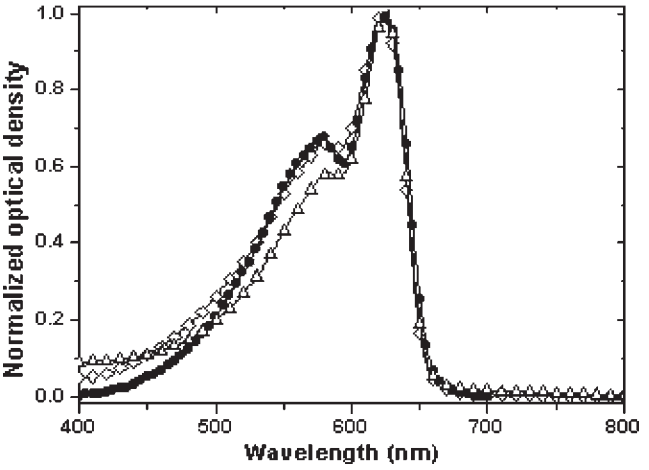

Figure 2. Normalized absorption spectra of 4B: (◇) evaporated film 200 nm with $X = 0.06$; (●) polymer crystal polarized perpendicular to the chain direction with $X = 1$; (△) isolated chains in a monomer crystal polarized parallel to the chain direction $X < 10^{-3}$.

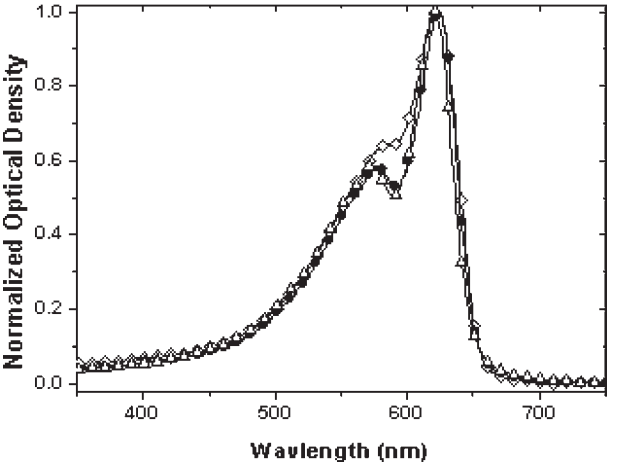

Figure 3. 4B evaporated film normalized absorption spectra for different polymer content X: (◇) $X = 0.023$, (●) $X = 0.23$, and (△) $X = 0.41$, 253 nm thick, irradiated with a Xe lamp.

content X of the film used. The absorptions of a film and of the solution obtained by dissolving it in chloroform were measured. The absorbance ε_{sol} of chloroform solutions of poly-4B is known.

The optical density OD_f of a film is $2.3OD_f = \alpha_{fp}^{(0)} X d$ and that of the corresponding solution $2.3OD_{sol} = \varepsilon_{sol} c l$, where l is the thickness of the cell containing the solution (here 10.0 mm) and c the molar concentration (mol L^{-1} if ε_{sol} is expressed in L mol^{-1} cm^{-1}). The total polymer mass present in the film is $m_p = S d \rho X$ where S is the irradiated film surface and ρ the density of the solid material.[29] So $c = m_p M/V$ where M is the molar mass and V the volume of solution. Hence

$$\alpha_{fp} = \varepsilon_{sol} \frac{OD_f S \rho l}{OD_{sol} V M} \qquad (1)$$

In this equation, all quantities relevant to the film can be accurately measured. The most demanding measurement is that of OD_f which may not be constant over the whole film surface. Irradiation of a total 15 × 15 mm^2 area was performed using the

xenon lamp. OD_f was obtained by averaging measurements taken through a 1 mm diameter hole at about 15 positions on the film surface. The combined uncertainties of all these parameters is estimated to be at most ±2%.

ε_{sol} was taken from the literature. There are three sets of data[36,48,49] with stated accuracies of ±5%, which differ slightly. The average 4×10^4 L^{-1} mol^{-1} cm^{-1} of the three values was used, but this is the main source of uncertainty in α_{fp}, which overall is known to ±5% or better.

Once α_{fp} is known, X can be deduced from OD_f of any film to the same accuracy. The final results correspond to unpolarized light propagating perpendicularly to the chains direction and through randomly oriented crystallites with lateral sizes and thicknesses comparable to or smaller than the wavelength of light.

The measurements on a film with $X = 0.4$ yielded

$$\alpha_{fp}^{(0)} = 2.62 \times 10^5 \text{ cm}^{-1}, \quad \alpha_{fp}^{(D)} = 1.53 \times 10^5 \text{ cm}^{-1}$$

The corresponding absorption cross section per repeat unit is $\sigma^{(0)} = 1.9 \times 10^{-16}$ cm^2/repeat unit using either the known poly-4B[30] or monomer[29] unit cells.

Absorption Spectra. The polymerization kinetics can be monitored by the time dependence either of the maximum optical density OD_{max} or that of the vibronic peak associated with the double-bond stretch vibration $OD(D)$ or of the area Σ under the spectrum which is proportional to the overall oscillator strength of the exciton transition including its vibronic satellites. These methods are equivalent as long as the spectrum shape is independent of polymer content X. Hence, the need of studying absorption spectra as a function of polymer content.

But this may be of interest for another reason, studying the influence of structural changes with polymer content in the mixed crystal on the chain electronic properties. This is very difficult with bulk single crystals, since the polymer absorption coefficients are very high, so the crystals become totally absorbing already at low X. This is no more the case with thin films.

The absorption of 4B films is unpolarized, corresponding to random orientation of the crystallites, the chain direction is parallel to the substrate surface. So the direction of the absorption transition moments is always parallel to the surface, but with random orientation. An example of absorption spectrum recorded at small X is compared in Figure 2 to those of isolated chains and polymer crystalline films prepared by the method described in refs 50 and 51 (spin-cast films are highly disordered and their absorption spectra are different). The latter two are both strongly dichroic, but the spectral shapes in polarization parallel and perpendicular to the chain direction are identical.[52] These spectra are typical of a blue PDA phase. So, microcrystals of monomer−polymer mixed crystal of 4B in our films are probably identical to the corresponding bulk crystals. No blue to red color transition is observed during photopolymerization at room temperature. However, the transition can be produced in the solid state by heating the film to a temperature smaller than the melting temperature of the mixed polymer−monomer crystal. Results will be reported elsewhere.

The shape of absorption spectra of 4B films is only approximately constant as shown in Figure 3 where spectra taken at an early stage, near the end of the reaction, and in between, are compared. Spectral changes are small but obvious, especially because the vibronic D band becomes well separated from the origin exciton band as reaction progresses.

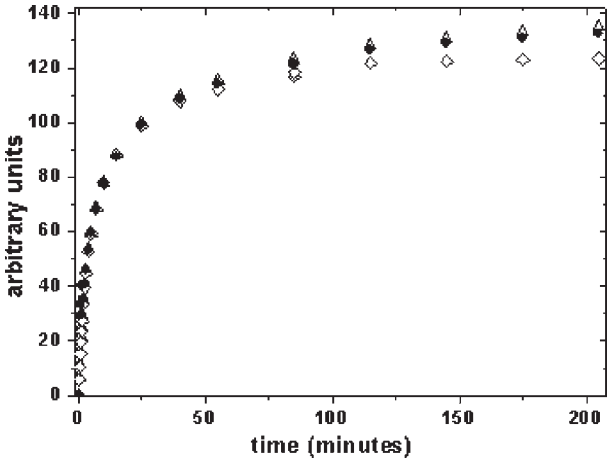

Figure 4. Example of changes with irradiation time of (◇) OD_{max}, (●) $OD(D)$, and (△) Σ of 4B evaporated film 253 nm thick, irradiated with a Xe lamp. Experimental values of OD_{max} and $OD(D)$ were scaled on Σ values to be equal at short time.

Spectral shapes may change for a variety of reasons: (i) changes in crystal quality will influence the inhomogeneous broadening, (ii) changes in chain geometry may affect the exciton energy or the Franck−Condon factor (FC) of the transition hence the ratios of zero-phonon to vibronic band intensities, and (iii) changes in the exciton coherence time or the exciton lifetime itself will influence the homogeneous broadening.

The changes with X of OD_{max}, $OD(D)$, and Σ are very similar except near the end of the kinetics where OD_{max} and to a lesser extent $OD(D)$ saturate ,whereas Σ keeps increasing slightly, possibly because some light scattering begins to occur due to incipient disorder. An example is given in Figure 4. So as a first approximation any of these may be used to characterize the kinetics.

The main spectral changes are at early stages a slight narrowing of the absorption bands, suggesting a decrease of inhomogeneous broadening (the ratio Σ/OD_{max} decreases by ~7% between $X \sim 0$ and 0.16, so use of OD_{max} slightly underestimates X in that range), and at higher X the appearance of a low-energy wing which may extend up to 800 nm . $OD(D)$ is initially not well-defined, until the vibronic absorption band is well separated from the exciton band, so $OD(D)$ cannot be used at early irradiation times. Considering these constraints, it was concluded that the best compromise will be to use OD_{max} to calculate the polymerization kinetics except at late times and $OD(D)$ except at early times.

λ_{max}, the wavelength corresponding to OD_{max}, also varies with X, first increasing significantly up to $X \sim 0.15$ and then decreasing smoothly up to the highest X. This needs to be understood in relation to structural changes, but it does not affect the determination of the kinetics. These data are discussed in the Appendix.

Line Shape Analysis. The improving resolution of the D-vibronic absorption band as X increases indicates a narrowing of the exciton (zero-phonon) line since the distance in energy of the two bands (the vibrational quantum energy in the excited state) stays approximately constant. Because of the presence of a phonon wing and remaining overlap with the D-band on the high-energy side, a line shape analysis of the origin exciton band is practical only on the low-energy side of the spectrum.

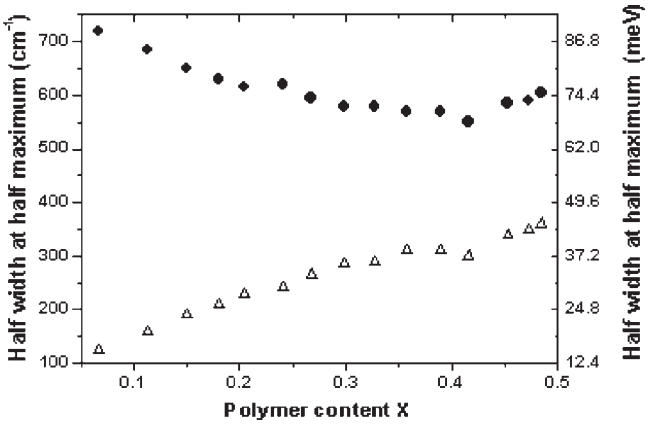

Figure 5. Variation of the half-width at half-maximum of (●) the Gaussian component w_G and (△) the Lorentzian component w_L with polymer content X used to fit the Voigt profile of the exciton line.

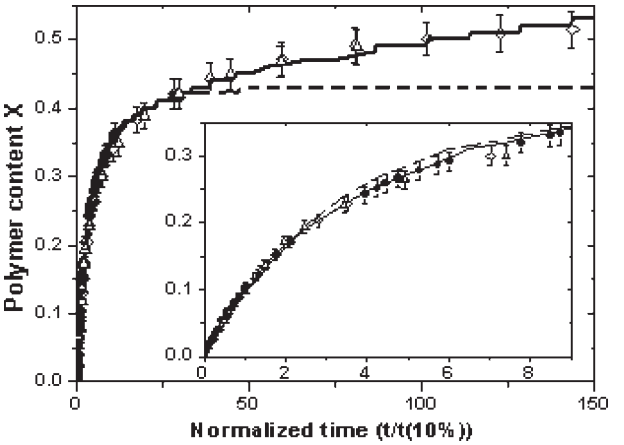

Figure 6. Kinetics of 4B normalized by the time needed to reach $X = 0.1$ obtained on evaporated films (◇) with the Cary lamp and $e = 253$ nm, (●) with the xenon lamp and $e = 253$ nm, and (△) with the xenon lamp and $e = 56$ nm. Numerical model (solid line) with $q = 0.1$, $p = 0.0015$, and $pp = 0.7$ and (dashed line) with $q = 0.1$, $p = 0$, and $pp = 0.7$. The error bars are ±5% of the data. The shape of the numerical model is a consequence of the discrete sampling.

The tail developing on the red side of the exciton band at high X suggested using a Voigt profile to fit the spectral region extending from a wavelength slightly lower than the maximum up to 800 nm. This profile is a convolution of a Gaussian representing the inhomogeneous broadening due to crystal inhomogeneities, by a Lorentzian corresponding to the homogeneous coherence time of the excitation, which may be due to exciton−phonon interactions, or to a very short exciton lifetime.

Except at small X where a single Gaussian correctly fits the whole line shape, with a half-width at half-maximum decreasing as X increases, convolution with a Lorentzian becomes necessary, and a Voigt profile well fits the studied spectral region (Figure 5). Results are very reproducible for different kinetics at the same temperature, and the fits are excellent.

The calculated Gaussian width w_G at very low X is in the range 100−115 meV, increasing slightly in between 14 and 28 °C; this is very close to the isolated chain value of 95 meV at 295 K.[52] It decreases to 70−80 meV as X increases to about 0.15 and then stays constant. The Lorentzian width w_L is always an increasing, slightly sublinear, function of X. The overall shape of its variation is independent of T, but its value near $X \sim 0$ is strongly T dependent between 14 and 29 °C where spectra were recorded. At the lowest T a Voigt fit is necessary even at the lowest polymer content, whereas above 20 °C a Gaussian fit is possible at small X. The largest value at the highest polymer content reached is $w_L \simeq 45-50$ meV.

Observation of a Lorentzian component indicates that the coherence time of the exciton shortens significantly as X increases. The maximum values of w_L correspond to a time ≤15 fs. This is 10 times smaller than the 135 fs exciton lifetime measured in isolated blue chains at low T.[53] One may then conjecture that the Lorentzian component corresponds to a very short exciton lifetime at room temperature and high enough X. Indeed, the blue exciton fluorescence quantum yield for isolated poly-4B chains at low T, though very small ($\sim 10^{-4}$),[10,54] is still at least 10 times larger than that of the pure polymer.[55]

Summarizing, these data suggest that the disorder in microcrystals is initially similar to that in the single crystal at the same temperature, and that their order somewhat improves during the first part of the polymerization, as the compressional stress on the chains disappears, probably by elastic deformation of the crystallites. In all that range, inhomogeneous broadening remains the major factor of line widths. Near $X = 0.15$, the chains are overall more ordered. Beyond this concentration, plastic deformation of the crystals sets in, possibly causing a small change in the chain geometry, corresponding to a slight increase of exciton energy and a shortening of the coherence time or of the actual exciton lifetime. The effect of such a deformation on exciton lifetime has not been studied theoretically.

The decrease of w_G in the mixed crystals (see Figure 5) implies a decrease in inhomogeneous broadening as X increases. In isolated chains, the exciton band broadens rapidly as T increases above ∼280 K,[6,52] implying a progressive disordering of the monomer crystal. Apparently, polymerization reduces or eliminates this disorder, at constant T. On the other hand, only a few broad Bragg peaks can be recorded from a poly-4B crystal.[30] However, its reflectance is still strongly dichroic,[56] so the disorder seen in diffraction does not seem to affect the parallelism of chains and does not apparently contribute to spectral inhomogeneous broadening. PDA chains may be more ordered than the medium in which they are embedded. There is no univocal relation between chain order and overall crystallographic order. This observation may be of interest for LB films and similar media.

Polymerization Kinetics and Reaction Rates. Several complete kinetics were registered on films with thicknesses ranging from 55 to 250 nm. Some much thinner films, close to a single monolayer, were also studied, with quite similar results, which will be reported later. All were prepared under the conditions described above. The irradiation times were normalized to the point corresponding to $X = 0.1$ using the measured film thicknesses and the absorption coefficient determined above. After normalization all kinetics fall on the same curve as shown in Figure 6 for a representative set of kinetics. The absolute value of X is known to ±10% only because the NRA cross section and $\alpha_{fp}(0)$ are determined to ±5% each. However statistical uncertainties are about 5% only so the different kinetics can be compared with that accuracy.

These data include irradiations using either the D lamp of the spectrometer or the Xe lamp. The fluxes of photons absorbed by

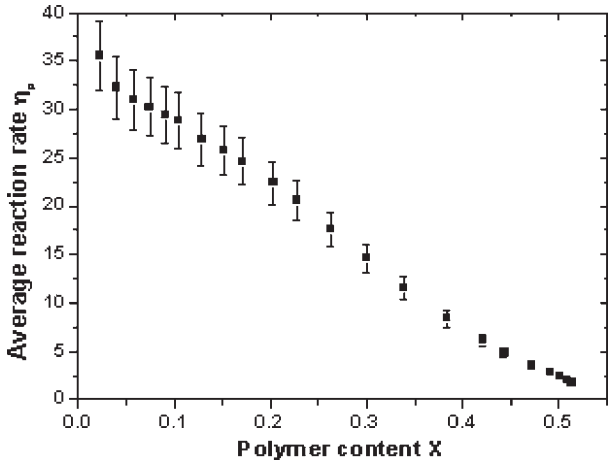

Figure 7. η_p average value obtained on a 4B evaporated film, of thickness 253 nm irradiated with a Xe lamp. Error bars 10% due to the systematic error on α the polymer absorption coefficient.

the monomer and active in photopolymerization differ by a factor 370. All fall on the same curve, indicating that there is no effect of the incident flux in that range.

The kinetics curve has two striking features: (a) It is not an exponential, meaning that the reactivity is dependent on the concentration of existing chains. (b) The reaction slows down to very small values beyond $X = 0.4$, contrary to what is observed in γ-ray-induced polymerization.

These data will now be used to estimate the reactivity of the 4B polycrystalline films and to model the kinetics. The reactivity can be quantified by the number η_p of monomers that are incorporated in a chain for one photon absorbed by the remaining monomer fraction in the film (photons absorbed by already existing chains are assumed to be ineffective). Two definitions of η_p are possible: (1) its "instantaneous" value, characterizing the increment δX produced by an irradiation time δt starting at a polymer content X: $\eta_p = (N_m/\alpha_m\phi)[(\delta X/\delta t)/(1 - X)]$, where N_m is the total number of monomers per unit volume. (2) A "mean" value to produce a polymer content X at time t starting from pure monomer to a mixed crystal with polymer content X, which corresponds to $\eta_p = X/(\int_0^t I_{abs}(t')\,dt') \propto X/(\int_0^t (1 - X(t'))\,dt')$. In the literature the mean value has been used. Values of mean η_p are shown in Figure 7, where the kinetics monoexponential, η_p, should remain constant. This is clearly not so; it tends to almost zero as X increases.

$\eta_p(X = 0) = 36$ is considerably less than in macroscopic single crystals.[34] The difference may reflect a large difference in chain lengths, as will be discussed now. The microscopically significant quantity is not η_p, but the probability η_i that a photon absorbed by a monomer molecule initiates a chain. The two quantities are related by $\eta_p = N\eta_i$, where N is the average number of repeat units in the chains so generated. As discussed above, N is expected to be nearly independent of X.

Within the assumption that any initiation produces a chain which length is equal to the length of the crystallite, any molecule excited within a stack of monomers will produce a chain of that length, if initiation indeed occurs. In other words, the probability that this stack of monomers will react is proportional to its N. The average is therefore a mass average number N_w. This is given by the GPC experiments as $N_w \sim 630$; hence, $\eta_i(X = 0) \sim 0.057$ close to the value 0.072 ± 0.015 found for single crystals,[34] in fact within the uncertainty of the latter value.

It was recalled above that at $X = 0$ there is a 1.4% mismatch, in the chain growth direction, between the monomer crystal and the relaxed polymer conformation, which disappears progressively. This produces a small change in the geometry of the reaction center, which might affect η_i. So, the experimental values of X at early times were compared to the optimized fit of the kinetic curve, and no difference was seen. If there is a variation of η_i it cannot be more than a few percent: the initiation probability from a neutral excited state in 4B is not sensitive to small changes in intermonomer distance.

As X increases, $\eta_i \rightarrow \sim 0$. This may result from either of two processes or a combination of both: (i) the excited state is quenched and its decay time shortens while the initiation rate constant does not change; (ii) structural changes in the b direction make initiation more and more difficult and the excited-state lifetime remains constant while the initiation rate decreases.

Origin of the Decrease of Initiation Rate. Understanding the kinetics of DA polymerization has been a long-standing problem.[16,17,57] We shall begin by considering the theoretical approach by Baughman, which has been very successfully applied to the thermal polymerization of pTS and similar DA,[25,26] and the model proposed by Prock et al.[32] in an early study of 4B photopolymerization. Also, Tieke[20] has proposed an empirical formula for kinetics. When they are adapted to our experimental conditions, none of them can account for our results. We shall then propose a model based on quenching of DA electronic excitations by transfer to existing chains and numerical calculations that account quantitatively for our observations.

Baughman's Model. Baughman investigated the effects of structural changes of the monomer−polymer mixed crystal as a function of polymer content during single phase thermal polymerization, in two different approximations. For DA crystals which undergo large dimensional changes in the reaction direction only (the case of pTS) he used the "crystal strain approximation": one considers a 1D line of monomers stacked in the chain growth direction, which therefore can be transformed in a polymer chain, and lateral interactions are neglected. This stack and the chain it generates both have the repeat distance of the average mixed crystal. The important parameter is a variation of the total free energy of the 1D system with average polymer content. For DA where dimension along the chain direction is essentially independent from conversion, he used the "nearest-neighbor approximation". In that case, there is no variation of the chain energy, but lateral interactions may modify the free energy of activation for initiation. Long-range interactions are neglected, while displacement of nearest neighbors on either lateral side of the reacting molecule dominates the free energy change. Effects on other nearby molecules within the reacting stack are neglected. 4B is close to the latter case: there is a small mismatch at zero conversion,[29] but the corresponding lattice parameter in the mixed crystal becomes quickly equal to the polymer value below ~ 0.2.[30] So the nearest-neighbor approximation will be used here. It contains several assumptions: (1) the initiation rate is independent of monomer−polymer conversion, (2) the rate of deactivation of the precursor species to initiation is independent of X and is much higher than the chain initiation rate, and (3) the active chain ends on growing chains have a characteristic lifetime which is independent of X.

These assumptions were chosen with thermal polymerization in mind. For instance, in assumption 2, the precursor species may

be viewed as a monomer molecule having transiently a vibrational energy content ≥1 eV. They are not well adapted to polymerization under irradiation where the precursor species has a characteristic, relatively long, lifetime. However, the theory has been shown to explain a variety of kinetic curve shapes, so its applicability to present data is worth examining.

The rate of solid-state polymerization reaction is given by (using Baughman notations)

$$\frac{dX}{dt} = BY(1-X)e^{-F_I/RT} \tag{2}$$

where B is a constant, F_I the part of the free activation energy for chain initiation which depends upon conversion, and Y the average length of chains formed near conversion X. In our case we may assume that all chains have the same length whatever the polymer content.

In the nearest-neighbor interaction approximation, the height W of the potential barrier at the transition state depends on whether 2, 1, or 0 lateral neighbors belong to a polymer chain, with values W_{pp}, W_{pm}, or W_{mm}, respectively. The free energy in the canonical ensemble can be written

$$F_I(X) = -RT\ln[X^2e^{-W_{pp}/RT} + 2X(1-X)e^{-W_{pm}/RT} + (1-X)^2e^{-W_{mm}/RT}] \tag{3}$$

if only the changes in intermolecular interaction energies for reacting monomer molecule are considered.

In a pairwise interaction approximation $W_{pp} = 2W_p$, $W_{mp} = W_m + W_p$, and $W_{mm} = 2W_m$. The origin of the energy scale can be selected for convenience so that $W_m = 0$. With this approximation eq 3 reduces to

$$F_I(X) = -2RT\ln(X(e^{-W_p/RT} - 1) + 1) \tag{4}$$

If we note $a = e^{-W_p/RT} - 1$, eq 2 becomes $dX/dt = BY(1-X)(aX + 1)^2$ with the initial condition at $t = 0$, $X = 0$, we find by integration

$$BYt = \frac{1}{1+a}\ln\left(\frac{aX+1}{1-X}\right) + \frac{aX}{1+aX} \tag{5}$$

Our experimental data can be fitted using such a relation, but considering that it corresponds to $a = -2$, which is not allowed by the definition of a, this fit has no physical meaning.

If instead of assuming Y constant, the form given by Baughman is used $Y = 2W_0^{-1}(1-X)^{1/2}$ the rate equation

$$\frac{dX}{dt} = 2BW_0^{-1}(1-X)^{3/2}(1-aX)^2 \tag{6}$$

with $a = 1 - e^{-W_p/RT}$ has again an analytical solution:

$$t = \frac{1}{P_1P_2^2}\left[3 - \frac{P_2}{1-X(1-P_2)}\sqrt{1-X} - 3 + P_2\right] + \frac{3\sqrt{1-P_2}}{P_1P_2^2\sqrt{P_2}}\left[\operatorname{atan}\sqrt{\frac{(1-P_2)(1-X)}{P_2}} - \operatorname{atan}\sqrt{\frac{1-P_2}{P_2}}\right] \tag{7}$$

with $P_1 = BW_0^{-1}$ and $P_2 = 1 - a$. No couple (P_1,P_2) can be found to fit the 4B kinetic curve.

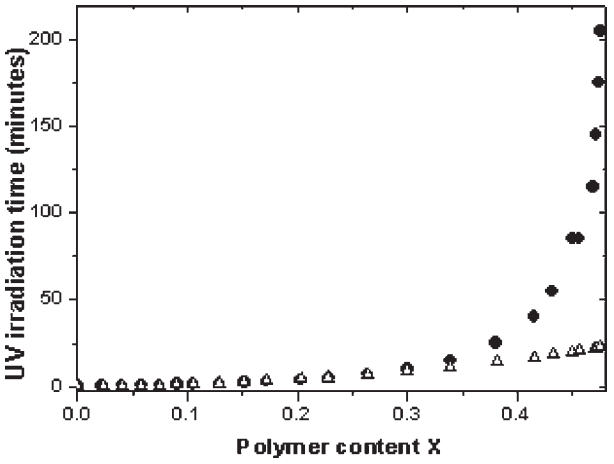

Figure 8. (●) Kinetics of 4B evaporated film 253 nm thick irradiated with a Xe lamp. (△) A fit with Prock's model with $kq = 15$ on 4B data up to $X = 0.3$.

In conclusion, Baughman's model cannot fit the present experimental situation. The most obvious reason is an X dependence of the initiation rate.

Prock's Model of 4BCMU Photopolymerization. To understand the photopolymerization reactivity of single crystal or films of 4B, Prock et al.[32] have introduced the notion of quenching of the initial excited state. The chain initiation probability q' (with Prock's notations) is now polymer content dependent due to a quenching by the existing polymer chains. The nature of this quenching is not detailed.

In ref 32, the differential equation governing the photopolymerization process is written

$$\frac{dX(x,t)}{dt} = Aq'I(x,t)(1-X(x,t)) \tag{8}$$

where A is a constant and $I(x,t)$ is the photon flux at time t and at a distance x from the surface into the crystal.

q' is written as $q' = q/(1+kX)$, where $q = \xi_i/(\xi_i + \xi_d)$, ξ_i is the chain initiation rate constant (not our probability η_i which is q'), ξ_d is the sum of rate constants of all other deactivation processes of the excited state, $k = \xi_q/\xi_d$ where ξ_q is the second-order rate constant of quenching by a polymer chain.

In the case of thin enough films, the x variable can be dropped, and the rate equation solution is analytical

$$t = -P_1\ln(1-X) - P_2X \tag{9}$$

with $P_1 = (1+k)/AI$ and $P_2 = k/AI$.

Figure 8 shows a fit to our data with $k_q = 15$, a value close to that found by Prock. The agreement is good up to $X \sim 0.3$ so he could rightly conclude that his model fitted his experimental data, but this is no more the case for more complete kinetics. It seems then that using a second-order rate constant may not be correct. Therefore, a numerical model has been developed, based on the idea of a quenching of neutral excited states.

Tieke's Formula. In order to calculate the polymer content in photopolymerized LB multilayers, Tieke[20] used the empirical formula $X = X(t=\infty)t/(a+t)$ assuming $X(t=\infty) = 1$. With this assumption the formula cannot account for our results. However, $X(t=\infty)$ may be taken as an adjustable parameter; this in fact assumes that photopolymerization can be incomplete, but it remains impossible to obtain a satisfactory two parameters fit of

our results. However, it is possible to fit the early part of the kinetics up to $X = 0.38$ with $X(t = \infty) = 0.46$, $a = 3.6$ implying that reaction stops at $X = 0.4$ which we know is incorrect. This underlines the need to extend the kinetics to times where polymerization has become very slow.

Numerical Model for Near-Neighbor Electronic Quenching by Polymer Chains. Polymerization nearly stops at $X \sim 0.5$. This suggests that the initiation probability of an excited monomer nearest neighbor to a polymer chain is zero or very small.

4B being a lamellar crystal, the distance between two monomers belonging to neighboring lamellae is 27.5 Å (see Scheme1). This is considered too long for quenching. The crystal will be assumed to be an addition of independent 2D systems. Within a lamella, chains grow along the **c** axis, and their distance along **b** is ~5.5 Å, allowing energy transfer. When one monomer initiates a chain, it is assumed that the chain grows to the full length of the crystallite along **c**. This has been observed experimentally in 4B microcrystals of sizes 300 nm to 1 μm prepared by the reprecipitation methods.[58] Polydispersity is not large; we assume that all chains have the same length. Therefore, the problem reduces to 1D: we consider a line of N monomers along the **b** axis, with cyclic boundary conditions.

A simple polymerization kinetic model with quenching by existent polymer chains has been computed. The probability of chain initiation is given depending on its environment: q is the probability if its nearest and second-nearest neighbors along **b** are not polymerized, p if one nearest neighbor is a polymer, $p/2$ if both are polymers, pp if only one second neighbor is polymerized, and $pp/2$ if both second neighbors are polymerized.

First a site is chosen at random, and its nature (monomer or polymer) is tested, if already a polymer another site is chosen; otherwise, its first neighbors nature is tested. A value s is chosen between 0 and 1 and compared to the probability q, $p/2$, or p following the results of the test on the nature of its first neighbor. If for example it has one first polymer neighbor and if $s < p$, the monomer is considered to have reacted and 1 is added to the polymer content; otherwise, 0 is added and another site is chosen. If a first neighbor is polymerized, no test is done on second neighbors. Now if the chosen site has no polymerized first neighbors, the existence of polymerized second neighbors is tested in the same way using the probabilities pp or $pp/2$. The total number of steps $M = 10^5$ is chosen to avoid edge problems. The time is the number of steps and the polymer content the sum of successful steps.

A set of (q, p, pp) triplets are tested to fit the experimental kinetics. To compare the numerical results, we normalize to the number of steps necessary to obtain 10% of polymer. The q value is chosen to have a reasonable number of steps to reach $X = 0.5$; here $q = 0.1$. In fact, it is a two-parameter $(p/q, pp/q)$ fit. Figure 6 shows the best fit to the data. It corresponds to $p/q = 1.5 \times 10^{-2}$ and $pp/q = 0.7$. Taking into account the nonstatistical uncertainties, p/q can be chosen in the range $[10^{-2}, 2 \times 10^{-2}]$ but $p = 0$ is excluded.

The quenching is almost total for monomers nearest neighbor to a chain and small for the second neighbor. Therefore, polymerization would be eventually completed at very long time, but this is not accessible because photodegradation would take over before.

Conclusion on 4B Photopolymerization. The main result of this study is that the reaction slows down dramatically beyond $X \simeq 0.4$ far from complete polymerization. Moreover, DO_{max} itself saturates at our longest irradiation time. This can be erroneously taken as an evidence for polymerization completion. A model incorporating quenching by monomer to polymer transfer accounts quantitatively for all kinetics. This energy transfer process should exist in all DA and particularly in LB films where intermolecular distances are close to 4B ones.[59,60] Therefore, the usual implicit assumption of complete final polymerization is likely to be wrong in many cases, and LB films too probably do not polymerize completely.

Calculations show a small quenching for the second neighbor of a polymer chain ($pp/q = 0.7$); this can be explained by the hopping of an electronic monomer excitation from a second neighbor to a first one or by a decrease of the initiation rate k_i. Whatever the main process is, it is a small effect for all polymer contents. Moreover, in the range $X \in [0, 0.15]$, k_i is independent of X while the intermonomer distance varies from 4.81[29] to 4.88 Å;[30] for $X > 0.15$, k_i is constant or decreases slightly if the diffusion is negligible. So the topochemical reactivity is not very sensitive to small geometric variations of active centers.

The inhomogeneous width of the exciton line and the exciton energy remain constant at high polymer content while disorder appears, enough to impede accurate crystallographic studies of the bulk polymer. This disorder has no effect on the chain conformation. So a small disorder does not prevent polymerization of 4B.

Some Results on 3B Photopolymerization Thin Films. Comparing 3B and 4B may be useful since these two DA have almost identical molecular formulas and similar crystal unit cells but very different reactivities. Therefore, some results on the photopolymerization of 3B thin films prepared in conditions identical to the 4B ones will be presented and discussed.

Absorbance of the Polymer in the Films. The method used was the same as for 4B. For 3B, $\varepsilon_{sol} = (43 \pm 2) \times 10^3$ L mol^{-1} cm^{-1} [36] and $\rho = 1.21$ g cm^{-3}.[29] The absorption coefficients measured on a film with $X = 0.08$ are

$$\alpha_{fp}^{(0)} = (2.85 \pm 0.30) \times 10^5 \ cm^{-1}$$

$$\alpha_{fp}^{(D)} = (1.82 \pm 0.08) \times 10^5 \ cm^{-1}$$

with the same uncertainty as for 4B due to the same possibilities of systematic errors. These values are not valid for all X in 3B where the spectrum changes significantly, as seen for instance by the ratio $\alpha_{fp}^{(0)}/\alpha_{fp}^{(D)}$, which steadily decreases as X increases. These changes and their consequences are discussed below. At small $X < 0.08$, $\alpha_{fp}^{(D)}$ is almost constant while $\alpha_{fp}^{(0)}$ decreases because the exciton absorption band broadens while its area remains nearly constant. This allows to calculate $\alpha_{fp}^{(0)}$ at $X \simeq 0$:

$$\alpha_{fp}^{(0)}(X \sim 0) = 4.5 \times 10^5 \ cm^{-1}$$

Note that $\alpha_{fp}^{(0)}(X \sim 0)$ is significantly larger than for 4B mainly because the exciton line width is smaller but also due to a 13% higher number of molecules per unit volume in the 3B monomer crystal.

Spectral Shape Analysis. In 3B, spectra at $X \leq 0.01$ are very well resolved (Figure 9) and identical to that of isolated chains in high-quality single crystals,[6,61] an indication that the films crystallites may have the same crystal structure and quality as macroscopic single crystals. As X increases, the $OD_{max}/OD(D)$ ratio rapidly decreases, and $OD(D)/\Sigma$ remains constant within a few percent up to $X \simeq 0.08$. Still in the same range the ratio of the area between the peak absorption wavelength and 800 nm, covering

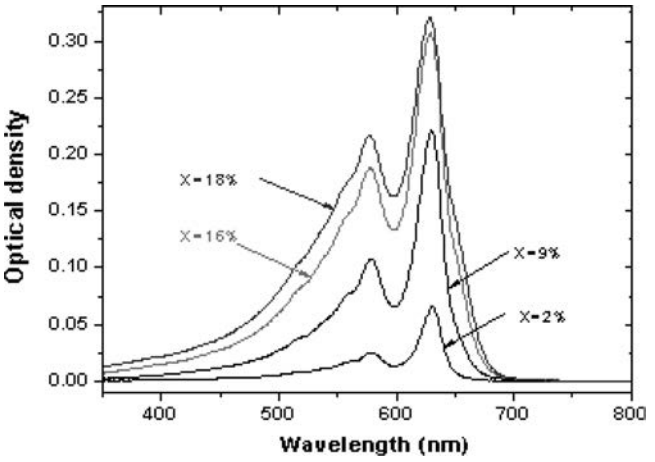

Figure 9. Absorption spectra of a 3B evaporated film, 150 nm thick with different polymer contents X upward X = 0.02, 0.09, 0.16, and 0.18 irradiated by a Xe lamp.

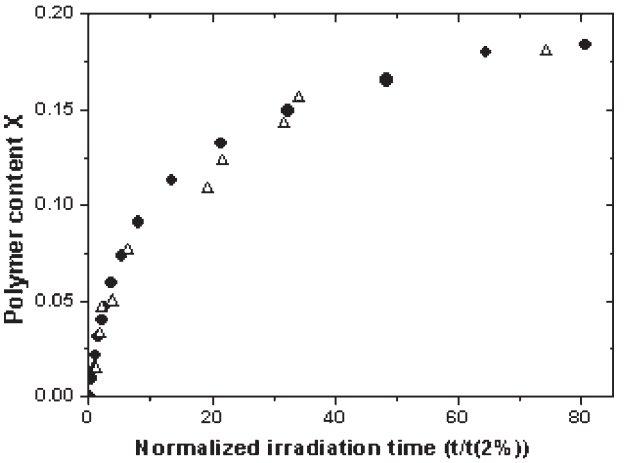

Figure 10. Photopolymerization kinetics of (●) a 3B evaporated film and (△) 3B very fine powders from ref 33 Figure 2. The time has been normalized to the time needed to obtain X = 0.02.

the low energy half of the exciton band, to the total area Σ remains constant, so the decrease of OD_{max}/Σ is due to the exciton line width variation.

In the same range, the line width is well fitted using a Voigt profile with a constant Gaussian line width w_G = 40 meV. The Lorentzian width is w_L = 26 meV at $X \sim 0$, and the convolution yields an effective width ~50 meV equal to that of isolated chains. w_L increases linearly with X up to ~55 meV at X = 0.08. The well-resolved spectrum and the constancy of w_G are consistent with a good and constant crystal quality.

Therefore, in this range of X either Σ or $OD(D)$, or even OD_{max} corrected for the line width variation, may all be used to determine the kinetics and the number η_p of monomers included in a polymer chain per absorbed photon, as shown below.

Beyond $X \sim 0.08$ this is no more true, as the overall spectrum changes in several ways:

(a) A weak shoulder grows around 655 nm, so the line shape may no more be accurately analyzed as above. But qualitatively the line keeps becoming broader at higher X, up to ~140 meV, and still looks like a convolution of a Gaussian and a Lorentzian with a tail extending toward the near-IR.

(b) An extra absorption appears at small wavelengths as a broad asymmetric band peaking near 530 nm at the expense of the exciton absorption and of the 655 nm band which both decrease. This may correspond either to a blue to red transition of existing chains or to direct formation of red chains. Red chains are known to occur as a minority population in 3B crystals even at very low polymer content.[9] If so, the corresponding absorption has to be taken into account in the polymerization kinetics. For all kinetics, X has been calculated using $OD(D)$ since at the corresponding wavelength the new absorption contributes. At very long irradiation times it may be better to correct the values by the variation of Σ.

Throughout these changes, λ_{max} decreases by less than 3 nm (i.e., the exciton energy increases by less than 9 meV). The exciton energy depends on the chain conformation (which determines the "bare energy") and the van der Waals correction due to variation of the surrounding medium polarizability. So, either both quantities are nearly independent of X or their variations compensate.

The partially polymerized films so obtained are not in equilibrium. When kept in the dark at room temperature for several tens of hours a broad band peaking near 500 nm, apparently distinct of the band at 530 nm mentioned before, appears and grows at the expense of the exciton absorption while the total area Σ remains constant within 2%. Upon further irradiation and further waiting time the absorption increases below ~400 nm, and it seems to correspond to the growth of a sloping baseline which may be due, not to yet another absorption, but to light scattering, meaning that the film becomes disordered. This introduces an uncertainty on the baseline so the last points of the kinetics may be slightly overestimated. All these changes need long waiting times. It may be conjectured that molecular diffusion is needed to plastically relax the structure. Elastic stresses near a surface can be relaxed by a plastic deformation increasing the surface area, due to surface diffusion of molecules. A diffusion distance of ~100 nm over a time $\sim 10^6$ s corresponds to a surface diffusion coefficient $\sim 10^{-16}$ cm^2 s^{-1}, a not unreasonable order of magnitude for a large molecule as a 3B monomer. For instance, the room temperature diffusion coefficient along grain boundaries in naphthalene, extrapolated from measurements at higher T[62] is $\sim 10^{-9}$ cm^2 s^{-1}.

Polymerization Kinetics. Comparison with 4B and Relation to Structural Changes. Figure 10 shows a 3B polymerization kinetics compared to a 3B UV kinetics of very fine powders obtained by grinding small crystalline flakes.[33] In the latter case the polymer content was determined gravimetrically. The excellent agreement between the two curves shows the accuracy of our α values.

Our 3B kinetics is then compared in Figure 11 to a 4B one, both films having the same thickness 253 nm and both being irradiated with identical flux. The polymer content of 3B, for a given dose, is much smaller. The initial slope of the two curve are different, they are determined by the η_p value which is in 3B $\eta_p = 2.7 \pm 0.5$ and in 4B $\eta_p = 36 \pm 0.5$. X is proportional to the dose up to X = 0.03; in this range η_p is constant and probably η_i also. In a 3B monocrystal,[34] $\eta_p \simeq 5$ while in microcrystalline film, chains have to be much smaller than in a monocrystal: the film reactivity is therefore larger. As absorption spectra of both type of samples are identical at low X, this difference is unlikely to be due to polymorphism. An obvious

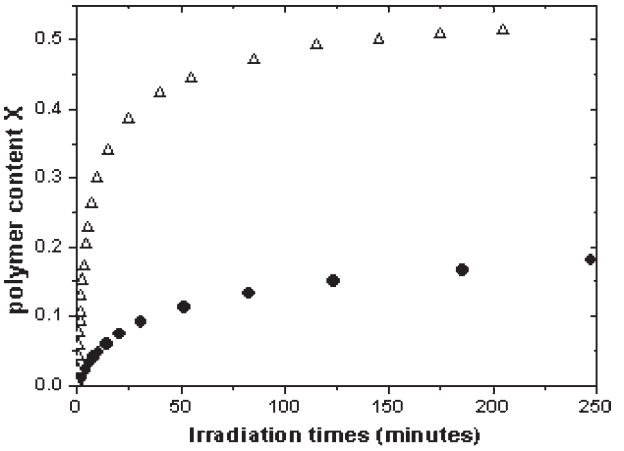

Figure 11. Kinetics of evaporated 253 nm thick films of (△) 4B and (●) 3B. The irradiation time of 3B has been corrected by the ratio of the 3B to 4B monomer absorbance to compare the reactivity.

difference between large monocrystals and thin films is the surface to volume ratio.

It is not possible to fit the 3B kinetics with the numerical model used for 4B. Even using a total quenching for the first and second neighbors the calculated kinetics does not slow down fast enough. One or more of the model hypotheses are not valid in 3B. Either η_i is no more constant and decreases as X increases or long-range quenching occurs which implies a substantial diffusion of the monomer excitation. The second possibility seems unlikely because the interstack distance in 3B is only 20% smaller than in 4B where diffusion is negligible. But the assumption of constant N can be questioned, too.

3B monomer crystals are generally of high enough quality to allow a complete crystal structure determination at room temperature.[29] 3B microcrystals are of similar quality since their absorption spectrum at $X \leq 1\%$ is practically identical to that of isolated chains.[6,61] In these crystals isolated chains are not strained since their repeat unit length is almost equal to the corresponding monomer crystal **b** parameter,[29] so it is expected that this parameter will not significantly change with X. However, one should not consider the geometry of the reacting center only; the deformation of the crystal produced by existing chains will affect the side groups as well. During an initiation or addition step side groups move, and if this motion is impeded by a neighboring group the reaction may not occur. Examples of DA crystals that are not reactive for that reason are known.[4] A similar situation may occur in partially polymerized 3B if the deformation of the mixed crystal will affect the geometry of unreacted monomers, particularly the side group packing. On the other hand, IR absorption studies to be reported elsewhere indicate that the H-bonds in 3B and 4B monomer crystals are very similar. This points to a role of the $-(CH_2)_n-$ spacers between the C≡C−C≡C group and the H-bonds in the initiation reactivity.

The polymer contents obtained here are much smaller than those reported for γ-polymerization of 3B.[35] For the latter, polydispersities M_w/M_n have been measured.[63] While in 4B they always are ≤3 and are comparable to those measured here, in 3B M_w/M_n remains small in the X range reached by UV: $M_w/M_n \sim 3$ at $X = 0.2$.[63]

But they increase enormously beyond $X \sim 0.2$: $M_w/M_n \sim 9$ at $X = 0.35$;[64] this corresponds to massive generation of very short chains and hence to problems with chain propagation. If the polydispersity is a function of X but not of the type of excitation, there is no such problem in the present study and the assumption that crystallite size determines the chain length remains valid.

An "even−odd effect" has been observed in PDA crystals, but it is generally related to the chains' electronic structure rather than to the polymerization (initiation) rate constant. In the BCMU family at least, the stable electronic structure of the chains is blue if n is odd and red if it is even, and it has been suggested that this is due to the parity of the spacer group favoring or not a planar conformation of the chain. Note that the poly nBCMU chains produced by polymerization of a crystal may be blue (as in the case of 4B), the red form being obtained for n even either by dissolution and reprecipitation of the polymer or by melting the polymer crystal,[65,66] or possibly upon thermal annealing of the solid phase. (A study of this color transition in the same 4B films as used in the present study is in progress.)

A similar odd−even effect has been observed in self-assembled monolayers of DA-thiols on Au[67,68] but not on early studies on LB multilayers of DA-acids.[24] But the length of the spacer (see, for instance, refs 39 and 69) and the nature of the subphase[39,70] are important as well, so it may not be easy to disentangle the effects. In LB films the blue to red transition is also often observed as polymerization proceeds (for a recent study see ref 70), and it is not clear if this transition has a large influence on the subsequent polymerization kinetics.

So what is known of the even−odd effect does not help much in understanding the behavior of 3B compared to 4B. It might be that the polymer including its side groups occupies a volume that is fairly different in shape from that of the monomer stack it replaces (see the concept of "reaction cavity" introduced by Cohen),[71] in which case large elastic stress will accumulate, leading to increasingly difficult initiation and propagation; in the language of Baughman's model the corresponding free energy for the reaction increases; a phase transition to a less reactive or unreactive phase is also possible. In fact, just the reverse, that is, the stress leading to a phase transition from a barely reactive phase to a more favorable one with consequently a great acceleration of the reaction is known in at least two DAs, DCH[72] and 1 EU.[73] This could be further elaborated only if structural information on partially polymerized 3B crystals was available.

■ CONCLUSION

A significant result of this work is the observation of a strong slowing down of photopolymerization rate, which may be assigned to the quenching of neutral excited states (precursor to initiation) by energy transfer to neighbor polymer chains. So, an apparent saturation of the reaction may not correspond to complete polymerization. This quenching may be expected to occur in LB films and similar structures, where the intermonomer distances are comparable to those in the studied compound.

This quenching of photopolymerization is observed in a material (4B) which polymerizes almost completely for γ-ray doses 15 Mrad. Therefore, quenching of ionic precursors to initiation must be much less efficient than for neutral ones. This remains an open question.

If quenching is not total but efficient ($p > 0$ in our model), total polymerization would in principle be attainable, but will not occur since photodegradation will take over. For total quenching ($p = 0$) polymerization will stop at $X \simeq 0.5$.

Our method to measure the absorption coefficient (α) without using gravimetry techniques needs soluble polymer. This coefficient depends on many parameters: number density of absorbing species, spectrum shape, and possible crystal optics effect, so these values are not directly useful for other DA. However a value of $\alpha = (3 \pm 0.5) \times 10^5$ cm^{-1} with a half-width at half-maximum on the excitonic band in the low energy side of $\sim$400 cm^{-1}, and assuming that the excitonic oscillator strength is almost the same for all PDA, can be used to give an order of magnitude of the polymer content in other DA.

This work is being extended to crystalline monolayers for a better comparison with Langmuir films in view and to the conditions for color transitions in the present and monolayer films.

APPENDIX. WAVELENGTH SHIFTS AND THEIR RELATION TO STRUCTURAL CHANGES

In PDA crystals, the exciton energy increases (λ_{max} decreases) under tensile strain in the elastic regime.[74] Similarly, at low polymer content PDA chains are under tensile or compressive strain due to the mismatch between the equilibrium repeat unit length of the chain ($\sim$4.9 Å) and the corresponding lattice parameter of the monomer−polymer mixed crystal (**c** for 4B). This mismatch, and the unit cell volume, are temperature dependent, so λ_{max} of the chains may vary for two reasons: variation of the strain and variation of the polarizability of the surrounding medium which causes a van der Waals correction to the electronic transition energies. This has been observed for isolated poly-4B chains dispersed in their monomer crystal matrix, which are under $\sim$1.4% compression at room temperature and 3.5% at 15 K: strain varies with T at constant X. Chains grow in the crystal along the **c** direction. Correspondingly, λ_{max} increases from about 625 to 685 nm.[75]

During polymerization the average crystal lattice parameters vary continuously from their monomer to their polymer crystal values if the reaction is homogeneous and does not occur via nucleation and growth of a polymer-rich phase. This is well documented in the case of the DA pTS (with side groups $CH_2-OSO_2C_6H_4CH_3$).[16,57,76] A study of 4B powder polymerized by X-ray irradiation[28] has shown the **c** parameter reaches the polymer value (4.88 Å[30]) well below $X \sim 0.2$. In the same range, the lateral area slightly decreases as it should for an elastic deformation. Beyond $X \sim 0.2$ **c** remains constant and the unit cell volume decreases significantly, corresponding to a plastic deformation.

The **c** increase leads to a decrease of the chain compressive strain and therefore an increase of the exciton energy (λ_{max} decreases). Simultaneously, the unit cell volume decreases; hence, the crystal polarizability increases and the rising chain concentration adds an extra contribution to it (the chains are more polarizable than the monomers). This entails an exciton energy decrease since it has been shown that the correction to excited state energies is always larger than that to the ground state, so larger polarizabilities lead to smaller transition energies.[77] Experimentally, λ_{max} in the films increases with X up to $X \sim 0.15$, which may indicate that in the 4B crystal the variation of polarizability dominates at room temperature; however, a variation of chain conformation cannot be excluded.

Beyond $X \sim 0.2$, λ_{max} starts decreasing. The volume contraction during isothermal polymerization is due to a decrease of the **b** lattice parameter by 3% from monomer to polymer while **c** has become almost constant. So there must be a plastic deformation of the crystal which may cause a (nonlongitudinal) deformation of the chain and side groups. We conjecture that the decrease of λ_{max} beyond $X \sim 0.2$ may result from such a deformation, but this cannot be further discussed pending structural data.

This sequence of events with increasing stress, first an elastic deformation, then a plastic one, and eventually rupture, is in fact typical and occurs in many materials (see for instance ref 78).

AUTHOR INFORMATION

Corresponding Author

*E-mail: sylvie.spagnoli@ujf-grenoble.fr (S.S.); michel.schott@insp.jussieu.fr (M.S.).

ACKNOWLEDGMENT

We thank E. Briand and I. Vickridge of INSP for their help with the NRA measurements within the cooperative structure around SAFIR at INSP and P. Pellat of LSP for helping in developing the computer program. We are grateful to G. Pembouong and F. Mathevet from Laboratoire de Chimie des Polymères, UPMC for the GPC measurements.

REFERENCES

(1) Wegner, G. *Z. Naturforsch.* **1969**, *24b*, 824–832.
(2) Baughman, R. H. *J. Appl. Phys.* **1974**, *43*, 4362–4370.
(3) Baughman, R. H.; Chance, R. R. *Ann. N.Y. Acad. Sci.* **1978**, *313*, 705–725.
(4) Enkelmann, V. *Adv. Polym. Sci.* **1984**, *63*, 91–136.
(5) Schott, M.; Wegner, G. In *Nonlinear Optical Properties of Organic Molecules and Crystals*; Chemla, D. S., Zyss, J., Eds.; Academic Press: London, 1987; Vol. 2, pp 3−49.
(6) Schott, M. In *Photophysics of Molecular Materials*; Lanzani, G., Ed.; Wiley-VCH: Weinheim, 2006; pp 49−151.
(7) Dubin, F.; Melet, R.; Barisien, T.; Grousson, R.; Legrand, L.; Schott, M.; Voliotis, V. *Nature Phys.* **2006**, *2*, 32–35.
(8) Legrand, L.; Al Choueiry, A.; Holcman, J.; Enderlin, A.; Melet, R.; Barisien, T.; Voliotis, V.; Grousson, R.; Schott, M. *Phys. Status Solidi B* **2008**, *245*, 2702–2707.
(9) Lécuiller, R.; Berréhar, J.; Lapersonne-Meyer, C.; Schott, M. *Phys. Rev. Lett.* **1998**, *80*, 4068–4071.
(10) Lécuiller, R.; Berréhar, J.; Lapersonne-Meyer, C.; Schott, M.; Ganière, J. D. *Chem. Phys. Lett.* **1999**, *314*, 255–260.
(11) Al Choueiry, A.; Barisien, T.; Holcman, J.; Legrand, L.; Schott, M.; Weiser, G.; Balog, M.; Deschamps, J.; Dutremez, S. G.; Filhol, J.-S. *Phys. Rev. B* **2010**, *81*, 125208(1−12).
(12) Schott, M. *J. Phys. Chem. B* **2006**, *110*, 15864–15868.
(13) Filhol, J.-S.; Deschamps, J. S.; Dutremez, G.; Boury, B.; Barisien, T.; Legrand, L.; Schott, M. *J. Am. Chem. Soc.* **2009**, *131*, 6976–6988.
(14) Reppy, M. A.; Pindzola, B. A. *Chem. Commun.* **2007**, 4317–4338.
(15) Yoon, S. L.; Kim, J.-M. *Chem. Soc. Rev.* **2009**, *38*, 1958–1968.
(16) Bässler, H. *Adv. Polym. Sci.* **1984**, *63*, 1–48.
(17) Sixl, H. *Adv. Polym. Sci.* **1984**, *63*, 49–90.
(18) Wegner, G. *Makromol. Chem.* **1971**, *145*, 85–94.
(19) Chance, R. R.; Patel, G. N. *J. Polym. Sci., Polym. Phys. Ed.* **1978**, *16*, 859–881.
(20) Tieke, B.; Wegner, G. *Makromol. Chem.* **1978**, *179*, 1639–1642.
(21) Fouassier, J. P.; Tieke, B.; Wegner, G. *Isr. J. Chem.* **1979**, *18*, 227–232.
(22) Alekseev, A. S.; Viitala, T.; Domnin, I. N.; Koshkina, I. M.; Nikitenko, A. A.; Peltonen, J. *Langmuir* **2000**, *16*, 3337–3344.
(23) Lopez, E.; O'Brien, D. F.; Whitesides, T. H. *J. Am. Chem. Soc.* **1982**, *104*, 305–307.
(24) Tieke, B.; Lieser, G. *J. Colloid Interface Sci.* **1982**, *88*, 471–486.
(25) Baughman, R. H. *J. Chem. Phys.* **1978**, *68*, 3110–3121.

(26) Baughman, R. H.; Chance, R. R. *J. Chem. Phys.* **1980**, *73* 4113–4125.
(27) Enkelmann, V.; Wenz, G.; Müller, M. A.; Schmidt, M.; Wegner, G. *Mol. Cryst. Liq. Cryst.* **1984**, *105*, 11–39.
(28) Brouty, C.; Spinat, P.; Sichère, M.-C.; Whuler, A. *Z. Kristallogr.* **1986**, *176*, 13–28.
(29) Spagnoli, S.; Schott, M.; Johnson, M.; Toupet, L. *Chem. Phys.* **2007**, *333*, 236–245.
(30) Brouty, C.; Spinat, P.; Whuler, A. *Acta Crystallogr. C* **1988**, *44*, 1070–1076.
(31) Patel, G. N. *Polym. Prepr. (Am. Chem. Soc., Div. Polym. Chem.)* **1978**, *19*, 154–157.
(32) Prock, A.; Shand, M. L.; Chance, R. R. *Macromolecules* **1982**, *15*, 238–241.
(33) Sottini, S.; Giorgetti, E.; Sparpaglione, M.; Brooks, D.; Licchelli, M.; Grando, D.; Skarda, V.; Westland, D. *Opt. Mater.* **1996**, *5*, 285–291.
(34) Schott, M.; Spagnoli, S.; Weiser, G. *Chem. Phys.* **2007**, *333* 246–253.
(35) Patel, G. N. *Radiat. Phys. Chem.* **1981**, *18*, 913–925.
(36) Spagnoli, S.; Berréhar, J.; Lapersonne-Meyer, C.; Schott, M.; Rameau, A.; Rawiso, M. *Macromolecules* **1996**, *29*, 5615–5620.
(37) Quillet, V.; Abel, F.; Schott, M. *Nucl. Instrum. Methods Phys. Res., Sect. B* **1993**, *83*, 47–61.
(38) Garbarz, J.; Lacaze, E.; Faivre, G.; Gauthier, S.; Schott, M. *Philos. Mag. A* **1992**, *65*, 853–861.
(39) Tieke, B.; Lieser, G.; Weiss, K. *Thin Solid Films* **1983**, *99* 95–102.
(40) Biegajski, J. E.; Burzynski, R.; Cadenhead, D. A.; Prasad, P. N. *Macromolecules* **1990**, *23*, 816–823.
(41) Rawiso, M., private communication.
(42) Campbell, A. J.; Davies, C. K. L. *Polymer* **1994**, *35*, 4787–4793.
(43) Liu, J.; Loewe, R. S.; McCullough, R. D. *Macromolecules* **1999**, *32*, 5777–5782.
(44) Wenz, G.; Müller, M. A.; Schmidt, M.; Wegner, G. *Macromolecules* **1984**, *17*, 837–850.
(45) Wegner, G. *Pure Appl. Chem.* **1977**, *49*, 443–454.
(46) Perkampus, H. H. In *UV-Vis Atlas of Organic Compounds*, 2nd ed.; VCH: Weinheim, 1992.
(47) Takabe, T.; Tanaka, M.; Tanaka, J. *Bull. Chem. Soc. Jpn.* **1974**, *47*, 1912–1916.
(48) Patel, G. N.; Chance, R. R.; Witt, J. D. *J. Chem. Phys.* **1979**, *70*, 4387–4392.
(49) Patel, G. N.; Khanna, Y. P.; Ivory, D. M.; Sowa, J. M.; Chance, R. R. *J. Polym. Sci., Polym. Phys. Ed.* **1979**, *17*, 899–903.
(50) Berréhar, J.; Lapersonne-Meyer, C.; Schott, M. *Appl. Phys. Lett.* **1986**, *48*, 630–631.
(51) Berréhar, J.; Hassenforder, P.; Lapersonne-Meyer, C.; Schott, M. *Thin Solid Films* **1990**, *190*, 181–197.
(52) Spagnoli, S.; Berréhar, J.; Lapersonne-Meyer, C.; Schott, M. *J. Chem. Phys.* **1994**, *100*, 6195–6202.
(53) Haacke, S.; Berréhar, J.; Lapersonne-Meyer, C.; Schott, M. *Chem. Phys. Lett.* **1999**, *308*, 363–368.
(54) Lécuiller, R.; Berréhar, J.; Ganière, J.-D.; Lapersonne-Meyer, C.; Lavallard, P.; Schott, M. *Phys. Rev. B* **2002**, *66*, 125205(1−6).
(55) Kobayashi, T. *J. Lumin.* **1992**, *53*, 159–164.
(56) Weiser, G.; Horvath, A. In *Primary Photoexcitations in Conjugated Polymers*; Sariciftci, N. S., Ed.; World Scientific: Singapore, 1997; pp 318−362.
(57) Bloor, D. In *Polydiacetylenes*; Bloor, D., Chance, R. R., Eds.; Martinus Nijhoff: Dordrecht, 1985; pp 1−24.
(58) Iida, R.; Kamatani, H.; Kasai, H.; Okada, S.; Oikawa, H.; Matsuda, H.; Kakuta, A.; Nakanishi, H. *Mol. Cryst. Liq. Cryst.* **1995**, *267*, 95–100.
(59) Tieke, B.; Lieser, G.; Wegner, G. *J. Polym. Sci., Polym. Chem. Ed.* **1979**, *17*, 1631–1644.
(60) Yanusova, L.; Klechkovskaya, V.; Sveshnikova, L.; Stiopina, N.; Kruchinin, V. *Liq. Cryst.* **1993**, *14*, 1615–1620.
(61) Lapersonne-Meyer, C.; Berréhar, J.; Schott, M.; Spagnoli, S. *Mol. Cryst. Liq. Cryst.* **1994**, *256*, 423–430.
(62) Sherwood, J. N.; White, D. J. *Philos. Mag.* **1967**, *16*, 975–980.
(63) Se, K.; Ohnuma, H.; Kotaka, T. *Polym. J.* **1982**, *14*, 895–905.
(64) Rawiso, M.; Aimé, J. P.; Fave, J. L.; Schott, M.; Müller, M. A.; Schmidt, M.; Baumgartl, H.; Wegner, G. *J. Phys. (Paris)* **1988**, *49*, 861–880.
(65) Iqbal, Z.; Murthy, N. S.; Khanna, Y. P.; Szobota, J. S.; Dalterio, R. A.; Owens, F. J. *J. Phys. C* **1987**, *20*, 4285–4292.
(66) Weiser, G.; Möller, S.; Horvath, A.; Lapersonne-Meyer, C.; Schott, M. *Proc. SPIE* **1997**, *3145*, 152–162.
(67) Menzel, H.; Mowery, M. D.; Cai, M.; Evans, C .E. *Macromolecules* **1999**, *32*, 4343–4350.
(68) Menzel, H.; Horstmann, S.; Mowery, M. D.; Cai, M.; Evans, C. E. *Polymer* **2000**, *41*, 8113–8119.
(69) Tachibana, H.; Yamanaka, Y.; Sakai, H.; Abe, M.; Matsumoto, M. *Macromolecules* **1999**, *32*, 8306–8309.
(70) Lifshitz, Y.; Upcher, A.; Shusterman, O.; Horowitz, B.; Berman, A.; Golan, Y. *Phys. Chem. Chem. Phys.* **2010**, *12*, 713–722.
(71) Cohen, M. D. *Mol. Cryst. Liq. Cryst.* **1979**, *50*, 1–10.
(72) Enkelmann, V.; Leyrer, R. J.; Schleier, G.; Wegner, G. *J. Mater. Sci.* **1980**, *15*, 168–176.
(73) Galiotis, C.; Young, R. J.; Ando, D. J.; Bloor, D. *Makromol. Chem.* **1983**, *184*, 1083–1101.
(74) Batchelder, D. N.; Bloor, D. *J. Phys. C: Solid State Phys.* **1978**, *11*, L629–L632.
(75) Spagnoli, S.; Berréhar, J.; Fave, J.-L.; Schott, M. *Chem. Phys.* **2007**, *333*, 254–264.
(76) Aimé, J.-P. Ph.D. Thesis, University Paris VII, 1984.
(77) Liptay, W. In *Modern Quantum Chemistry, Part 2*; Sinanoglu, O., Ed.; Academic Press: New York, 1965; p 173.
(78) Kelly, A.; Macmillan, N. H. In *Strong Solids*; Oxford Science Publ.: Oxford, 1986.